PHYSICAL REVIEW B VOLUME 19, NUMBER 8 15 APRIL 1979

Electronegativity scale for metals

J. A. Alonso* and L. A. Girifalco
Department of Metallurgy and Materials Science and the Laboratory for Research on the Structure of Matter, University of Pennsylvania, Philadelphia, Pennsylvania 19104
(Received 25 September 1978)

A model for alloy formation is used in which the electrochemical or charge-transfer effects are governed by the difference in the electronic chemical potential μ of the pure metals, provided that the pure metals are previously expanded or compressed in order to have the same electron density ρ_b at the boundary of the atomic cells. Then, a comparison of the curves $\mu = \mu(\rho_b)$ corresponding to different transition metals reveals that the curves are parallel and that $\Delta\mu$ is almost independent of ρ_b. This permits us to characterize each metal by one "electronegativity" parameter, and the scale obtained correlates well with the empirical scales of Pauling and Miedema. It also explains why the same set of electronegativity parameters describes liquid and solid alloys in Miedema's empirical theory of heats of formation.

I. INTRODUCTION

The study of the physical factors responsible for alloy formation is a topic of much current interest. Miedema[1] and co-workers have proposed a successful empirical formula that correctly predicts the sign, and gives semiquantitative results, for the magnitude of the heat of formation ΔH of binary alloys. The formula is

$$\Delta H = [-P(\Delta\phi^*)^2 + S(\Delta\rho_b^{1/3})^2] f(c), \quad (1)$$

where ρ_b is the electron density at the boundary of an atomic cell in the pure metal, ϕ^* is an electronegativity parameter, approximately equal to the work function and Δ indicates the difference between the two metals. P and S are universal constants and $f(c)$ is a function of the concentration. The success of Miedema's formula offers a natural guide for theoretical work; its relation to more fundamental descriptions of alloy formation has been attempted elsewhere.[2-4] In this paper we investigate in detail the origin of the negative term in Eq. (1). By using a microscopic description of the alloying process that permits us to separate ΔH into several contributions with a clear physical interpretation, the mechanism and parameters responsible for the so-called "electrochemical" or "charge-transfer effect" can be identified. Also the origin of the positive term in Eq. (1) appears naturally, although that positive term is not the subject of this work. As the main result of the paper, a theoretical electronegativity scale is derived for transition metals that correlates well with the empirical scales of Pauling and Miedema and gives a sound basis for their success. Qualitative consequences about the charge transfer are derived that agree with the results of the few full quantum-mechanical calculations available at present.

II. ALLOY FORMATION AND CHARGE TRANSFER

Alloy formation can be qualitatively understood by using a process proposed by Hodges and Stott[5] in the context of the energy density functional formalism.[6] We have modified[4] slightly that process in order to overcome some difficulties derived from the nonlocality of the energy density functional. The new process, divided in three steps, is as follows (we consider an equiatomic binary alloy):

(i) Start with the pure metals A and B, with atomic volumes V_A and V_B, and compress or expand them to the point at which the two following conditions are fulfilled: First, $\rho^p_{b,A} = \rho^p_{b,B}$, where $\rho^p_{b,A}$ and $\rho^p_{b,B}$ are the average electron densities at the surface of the atomic Wigner-Seitz cells of the transformed metals. Second, $\frac{1}{2}(V^p_A + V^p_B) = V_{\text{alloy}}$, where V_{alloy} is the experimental volume per atom of the alloy, and V^p_A and V^p_B are the atomic cell volumes of the transformed metals, that we will call "prepared metals". For a given V_{alloy}, these two conditions define unambiguously the prepared cells (note that for a given metal, and within the Wigner-Seitz sphere approximation, a one-to-one correspondence exists between atomic volume and electron boundary density). The elastic energy per atom needed to transform the pure metals is

$$E_{\text{el}} = (1/4V_A X_A)(V^p_A - V_A)^2 + (1/4V_B X_B)(V^p_B - V_B)^2, \quad (2)$$

where X_A and X_B are the compressibilities. E_{el} accounts for the positive term in Eq. (1).

(ii) Cut up the two prepared metals into atomic cells and fit the cells together in the crystallographic array of the alloy, maintaining the electron density unchanged within each cell. At this moment the electron distribution is not the alloy

ground-state distribution and the electronic chemical potentials μ_A and μ_B in the A- and B-type cells are different. Actually a small change in the shape of the prepared cells will be necessary in order to fill the space. Although the energy corresponding to this "structural" change can be neglected in general in the calculation of ΔH (except where ΔH is very small), it can be very important to explain the crystallographic structure of the alloy.

(iii) Because of the fact that μ_A and μ_B are not equal, electronic charge will be transferred from the cells with larger μ, to the cells with smaller μ in order to make the chemical potential constant everywhere. Hodges and Stott[5] have demonstrated that the electrochemical energy per atom liberated by the transfer of charge is

$$E_{ec} = -Q(\mu_A - \mu_B)/4, \tag{3}$$

where Q is the charge transferred to (or from) each cell.[7] E_{ec} favors alloy formation.

A key point is how to approximate μ_A and μ_B, the electronic chemical potentials in the A and B cells of the alloy before the electron relaxation takes place. The simplest approximation is to use for μ_A and μ_B the values $\bar{\mu}_A$ and $\bar{\mu}_B$ of the prepared metals. Nevertheless, this is not exact as can be seen starting with the definition of $\mu(\vec{r})$,

$$\mu(\vec{r}) = \delta E[\rho]/\delta\rho(\vec{r}), \tag{4}$$

and noticing the two following facts: first, $E[\rho]$ is a nonlocal functional of the electron density and second, the atomic environments around an A-type cell in the alloy and in the metal are different. The main corrections $\Delta\bar{\mu}_A$ and $\Delta\bar{\mu}_B$ to $\bar{\mu}_A$ and $\bar{\mu}_B$ have the form[4] of a Madelung potential. Then, Eq. (3) takes the form

$$E_{ec} = -Q(\bar{\mu}_A - \bar{\mu}_B)/4 - \sum_{i \neq j} Q^2/r_{ij}\,. \tag{5}$$

One expects Q to be proportional[1,4,5,8] to $(\bar{\mu}_A - \bar{\mu}_B)$. Then, Eq. (5) has the form of the negative term in Eq. (1). Equation (5) recovers a useful interpretation: E_{ec} is governed by the electrochemical potentials of the pure "prepared metals" $\bar{\mu}_A$ and $\bar{\mu}_B$ as one would expect, and it contains a Madelung term which depends on the structure and degree of order.

III. ELECTRONIC CHEMICAL POTENTIAL AND ELECTRONEGATIVITY

Because of the fact that $\bar{\mu}_A$ and $\bar{\mu}_B$ are the critical parameters determining the charge transfer and the electrochemical energy, a comparison of the curves $\mu = \mu(\rho_b)$ for different metals (note that the prepared cells have a common boundary density ρ_b) should rationalize the charge transfer in alloys and should give theoretical support to the empirical electronegativity scales.[1,9] This is in fact true as will be seen in this section.

The function $\mu = \mu(\rho_b)$ for each metal will be constructed from the following two functions: first, the function $\mu = \mu(R)$, where R is the Wigner-Seitz radius, and second, the function $R = R(\rho_b)$. We start by considering $R = R(\rho_b)$. We used a modified Thomas-Fermi-Dirac method in previous works,[10-12] which provides a simple and accurate way to obtain the electron density in the atomic cell for any Wigner-Seitz radius of the metal, and the electron density at the cell boundary. We do not give details of the method here but only say that, in order to compute the electron density, the knowledge of the electronic configuration (that is, the occupation number of the valence levels) of the metal is needed. Only transition metals are treated in this paper, their electronic configurations taken from the calculations made by Nieminen and Hodges,[13] showing good agreement with other very accurate calculations.[14] Our results for the function $\rho_b = \rho_b(R)$ for the $3d$ and $4d$ transition metals are presented in Fig. 1. For Mn, Tc, and Ru, metals for which Nieminen and Hodges do not give electronic configurations, these were estimated from a comparison between the configurational trends shown in the Nieminen-Hodges paper and in other works.[14,15] Then we used the following configurations for these metals: Mn ($d^{5.7}s^{1.3}$), Tc ($d^{5.8}s^{1.2}$), and Ru ($d^{6.8}s^{1.2}$). For Zn and Cd it was assumed that the electronic configuration in the metal is the same as in the free atom, i.e., $d^{10}s^2$. Some trends are apparent in Fig. 1. (a) At a given R, ρ_b is greater for the $4d$ metals, a consequence of the bigger noble gaslike core. (b) In each of the two series, at a given R, ρ_b roughly decreases as the atomic number increases (some exceptions occur in the $4d$ series). This is understandable because, in each series, as the number of d electrons increases, the localization of the d-wave functions increases. Because of the fact that the electronic configuration used for each metal corresponds to the equilibrium R of that metal, the curves are less reliable for values of R far from the equilibrium value.

The second function that we need is $\mu = \mu(R)$. A local approximation is not adequate.[4] For a given R, μ can be calculated[13] from band-structure parameters, as

$$\mu = E_F - V_c = E_F - V_0 + V_{xc}\,, \tag{6}$$

where E_F is the Fermi energy, V_c is the average coulombic potential at the cell boundary, i.e., the average cell-boundary potential V_0 minus the exchange-correlation contribution V_{xc}. Normally the

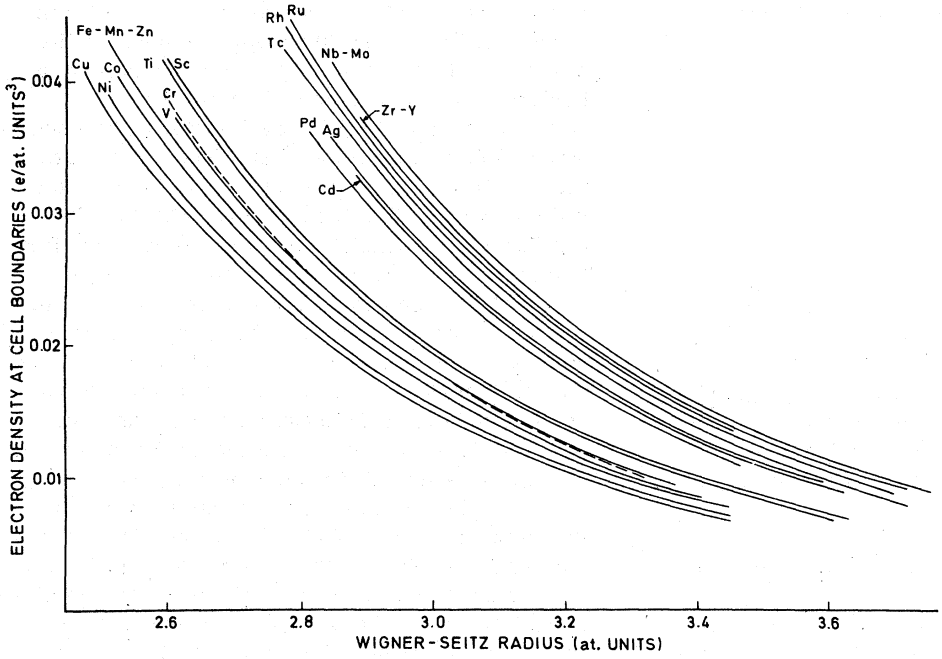

FIG. 1. Electron density at the boundary of atomic cells as a function of the Wigner-Seitz radius for the $3d$ and $4d$ transition metals.

band calculations give these quantities in the muffin-tin approximation. Only a few band calculations as a function of the lattice parameter have been published. Taking the data from them,[16] we have plotted $E_F^* = E_F - V_0$ vs R in Fig. 2 for the metals V, Y, Nb, Tc, and Ag. We did not include the contribution of V_{xc} in the figure for reasons that will become clear later. Finally from Figs. 1 and 2 we have constructed the functions $E_F^* = E_F^*(\rho_b)$ and plotted them in Fig. 3. The curves for Mo and Cu are also plotted. For these two metals, E_F^* as a function of R was taken from Williams.[17] The reason the V_{xc} contribution in Eq. (6) was not included in plotting Figs. 2 and 3 is that the band structure calculations normally use a local approximation for the exchange-correlation potential; in these circumstances, at the cell boundary

$$V_{xc} = -3\alpha(3\rho_b/8\pi)^{1/3}, \tag{7}$$

and therefore V_{xc} only depends on the cell-boundary electron density. (We assume that the same value of the constant α is valid for all the metals; $\alpha = \frac{2}{3}$ is the value generally accepted.) Thus in the calculation of $(\mu_A - \mu_B)$ in Eq. (5), the V_{xc} contributions cancel because the electron density at the boundary of A cells is the same as for B cells. Then the use of V_{xc} will add to all the curves the same function of ρ_b and $\Delta\mu(\rho_b) = E_F^*(\rho_b)$. Although

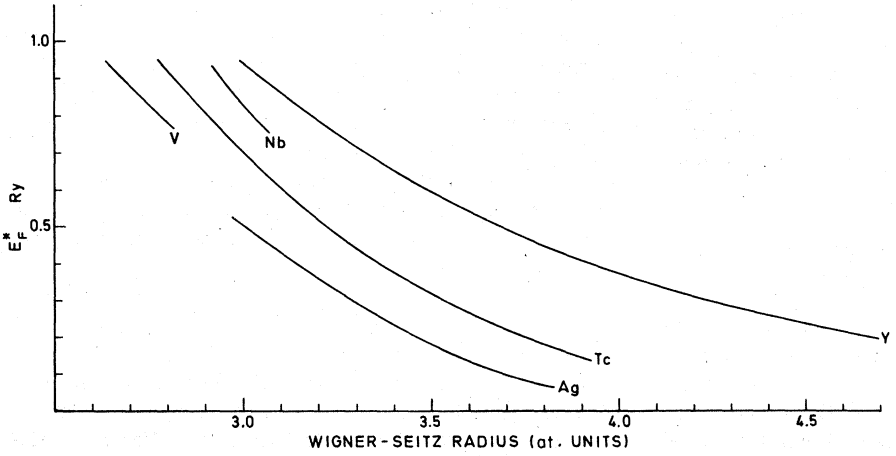

FIG. 2. Fermi energy (measured with respect to the total crystal potential at the atomic cell boundary) versus Wigner-Seitz radius.

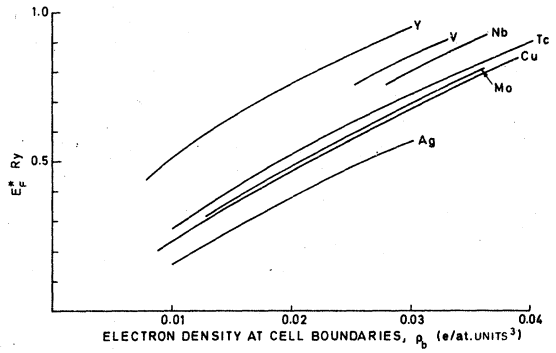

FIG. 3. Fermi energy (measured with respect to the total crystal potential at the atomic cell boundary) versus the electron density at the cell boundary.

the exchange-correlation potential is in the local-density approximation, the resulting μ is, of course, nonlocal since it results from solution of the Schrödinger equation. The effect of the local V_{xc} on μ is not known, but the local-density approximation is successful for solid-state band theory calculations. It is only the difference $\Delta\mu(\rho_b)$ that is important here. The main observation about Fig. 3 is that the curves are approximately parallel and the value $\Delta\mu = E_{F,B}^*$ is almost independent of ρ_b (at least for values of ρ_b that are not very small). This fact will be exploited to interpolate the curves corresponding to the metals for which only one point of the curve is known, the point corresponding to the equilibrium volume. This was done by drawing a curve through the one point that is parallel to the closest curve whose $E_F^*(R_s)$ is known.

We recall that the prepared cells have equal boundary density and that the driving force for the transfer of electrons between A and B cells is the difference $\Delta\mu$ taken at the appropriate ρ_b. μ changes with ρ_b, but the fact that the curves for different metals are approximately parallel and $\Delta\mu$ is nearly independent of ρ_b makes it possible to define a unique number $\Delta\mu$ for each pair of metals or, in other words, makes it possible to characterize each curve with an "electronegativity" parameter. We believe that this fact connects with the empirical descriptions of the electronegativity and explains why such an "electronegativity scale" can be defined and why the electrochemical effect[1,7,18] in alloys can be expressed in terms of the electronegativity difference. Also, the independence of $\Delta\mu$ on ρ_b is, in our opinion, the fact that explains why the same set of electronegativity parameters describes solid and liquid alloys in Miedema's theory.[19] The volume of a binary liquid alloy is greater than the volume corresponding to the solid alloy of the same concentration. That greater volume implies greater volumes of the prepared cells at the end of step (i) in Sec. II, and consequently, a smaller boundary density ρ_b. Nevertheless, even if ρ_b decreases, $\Delta\mu$ has the same value as for the solid case.

With these ideas in mind we have plotted in Fig. 4 the equivalent of Fig. 3 but including all the transition metals of the $3d$ and $4d$ periods (including the Cu and Zn groups) plus a few $5d$ metals. In order to make Fig. 4 clear, only the curves corresponding to V, Cu, Ag, and Pd were plotted. For the rest, only one point is plotted and the interpolation of the corresponding curve can be easily made. Figure 4 was constructed in the following way: the value of E_F^* corresponding to the point characterizing each metal (that point is plotted as a cross in Fig. 4) was taken from the

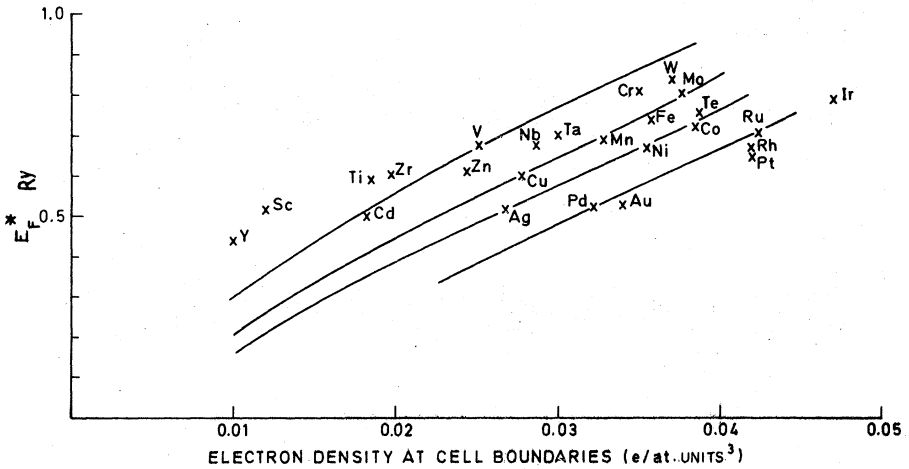

FIG. 4. Same as Fig. 3, but including all the $3d$ and $4d$ transition metals and some $5d$ metals. Only a few curves are plotted (V, Cu, Ag, and Pd) to make the figure clear and the restant curves can be easily interpolated through the points corresponding to other metals. See the text for details on the construction of the figure.

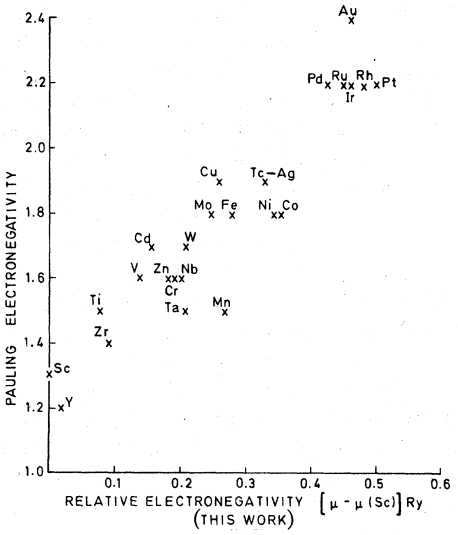

FIG. 5. Comparison between the relative electronegativity scale of this work and the Pauling scale.

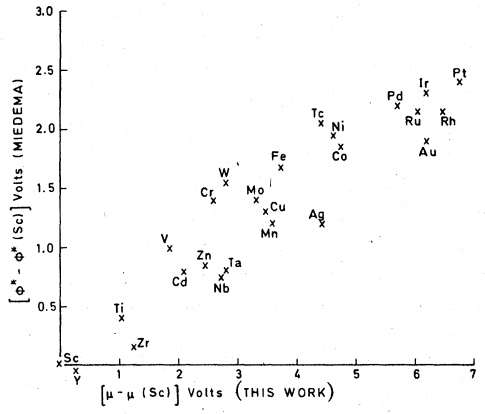

FIG. 6. Comparison between the relative electronegativity scale of this work and the scale of Miedema. Sc is taken as zero for both scales.

self-consistent band calculations made by Papaconstantopoulos *et al.*[20] The corresponding value of ρ_b (i.e., the value of ρ_b that corresponds to the value of R at which the band calculation was made) was, as before, taken from Fig. 1. Then, the curves in Fig. 4 (V, Cu, Ag, and Pd) were constructed by drawing curves parallel to the curves of Fig. 3 and passing through the cross points corresponding to V, Cu, Ag, and Pd, respectively. Plotting Fig. 4 from a set of band calculations,[20] all using the same method and approximations, makes Fig. 4 more realistic than Fig. 3, in which results from rather different methods were used. This can be important for the values of $\Delta\mu$. In plotting the points corresponding to the 5*d* metals (Ta, W, Ir, Pt, and Au) the values of ρ_b and E_F^* were taken from Neiminen and Hodges[13] because no other values were available. In the analysis of the results of Fig. 4 one must have in mind the fact that the 5*d* metals do not correspond to the same kind of calculation as the others. Alkaline and alkali-earth metals were not included because the typical values of ρ_b in these metals are much smaller than in transition metals, and it is not evident how to extrapolate the transition metal curves to those small values of ρ_b. Work on this point is in progress.

IV. ELECTRONEGATIVITY SCALE IN COMPARISON WITH OTHERS

The ordering of the curves in Fig. 4 (only a few curves are plotted, for clarity of the figure) gives a first-principle relative-electronegativity scale.

TABLE I. Calculated electronegativity scale, $\mu - \mu$(Sc) with Sc is taken as zero.

Metal	Relative electronegativity (Ry)	Metal	Relative electronegativity (Ry)
Sc	0	Mn	0.27
Y	0.02	Fe	0.28
Ti	0.07	Tc	0.33
Zr	0.09	Ag	0.33
V	0.13	Ni	0.34
Cd	0.15	Co	0.35
Zn	0.18	Pd	0.42
Cr	0.19	Ru	0.45
Nb	0.20	Ir	0.46
W	0.21	Au	0.46
Ta	0.21	Rh	0.48
Mo	0.24	Pt	0.50
Cu	0.26		

With the values of $\Delta\mu$ calculated from the curves, and taking Sc as our zero of electronegativity, the theoretical scale is compared with the scales of Pauling[9] and Miedema[21] in Figs. 5 and 6. The calculated relative electronegativities are given in Table I. A good linear correlation is found with each of the two scales. The linear correlation is, in fact, as good as the correlation existent between the scales of Pauling and Miedema. We do not claim improvement over these scales and this is not the purpose of our calculations. Rather, the fact that the scale derived here from first principles correlates well with the empirical scales provides a firm physical basis for the latter ones. The correlation between the theoretical scale and the Mulliken[22] electronegativity scale is less satisfactory. This can be understood because the Mulliken scale is derived from free-atom parameters, while the Pauling and Miedema scales are derived from solid-state properties as well as the scale of this paper. In Fig. 7 it is seen that the theoretical electronegativity also correlates linearly with the experimental work function[22] ϕ. The linear function is roughly

$$\mu - \mu(\mathrm{Sc}) = 2.75[\phi - \phi(\mathrm{Sc})]. \tag{8}$$

The same constant 2.75 describes the linear correlation with the scale of Miedema. This is expected because the parameters ϕ^* obtained empirically by Miedema are close to the experimental work functions.

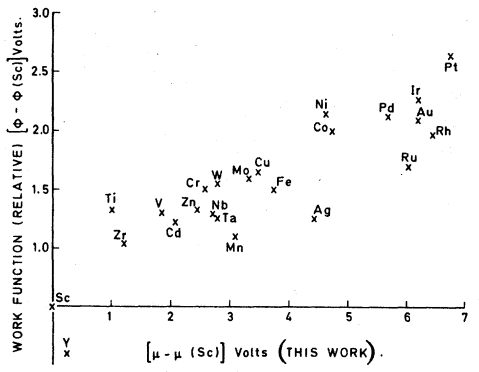

FIG. 7. Comparison between the relative electronegativity scale of this work and the experimental work function. Sc is taken as zero for both scales.

V. COMMENTS ON THE CHARGE TRANSFER

In Fig. 4 the charge transfer between two metals is from the metal with the higher curve to the metal with the lower curve. Considering the position of the curves for Cr, Mo, and W, we see that the transition metals to the right of the Cr group in the Periodic Table correspond to the low curves in the figure, whereas the elements to the left of the Cr group have high curves. Then, in forming alloys, the elements to the left of the Cr group will transfer charge to the elements at the right, in agreement with the predictions of Beck[23] and with detailed band-structure calculations.[24-26] As noted by Miedema,[27] this fact is in disagreement with the Engels-Brewer theory.[28] Our predictions can be also checked with work in other alloys. The direction of the charge transfer agrees with the calculations of Yamashita *et al.*[29] (Fe and Co) and Moruzzi *et al.*[30,31] (ZnNi and ZnCu). Watson and co-workers[32] have studied the charge transfer in dilute gold alloys with Pd, Pt, Ni, and Ag. They found a net charging at the Au sites, the charging being close to zero in the Pt alloy. This is consistent with Fig. 4, where Au is found to be more electronegative than Ag, Pd, and Ni. Also Au and Pt are found to have very close electronegativity, although Pt appears to be slightly more electronegative. This small discrepancy can perhaps arise from the approximations involved in the construction of Fig. 4. We note, nevertheless, that Pt is also more electronegative than Au in the scale of Miedema.

The results of this paper would probably improve if both functions, $\rho_b = \rho_b(R)$ and $\mu = \mu(R)$ are obtained from the band calculations as a function of the lattice parameter. When more of these become available, our understanding of the electrochemical effects in alloys will improve, and the ultimate goal of predicting the properties of the alloy in terms of parameters corresponding to the pure component metals will be closer.

ACKNOWLEDGMENTS

We acknowledge stimulating discussions with Dr. A. R. Williams and Dr. C. D. Gelatt. We also thank Dr. A. R. Williams for making available to us his results for band-structure parameters as a function of lattice constant in some metals. This work was supported by the NSF through the University of Pennsylvania Materials Research Laboratory under Grant No. DMR-76-00678.

*Present address: Fisica Teorica, Facultad de Ciencias, Universidad de Valladolid, Valladolid, Spain.
[1]A. R. Miedema, J. Less Common Met., 46, 67 (1976) and references therein.
[2]C. H. Hodges, J. Phys. F 7, L247 (1977).
[3]J. Chelikowsky and J. C. Phillips, Phys. Rev. B 17, 2453 (1978).
[4]J. A. Alonso and L. A. Girifalco, J. Phys. F 8, 2455 (1978).
[5]C. H. Hodges and M. J. Stott, Philos. Magn. 26, 375 (1972).
[6]P. Hohenberg and W. Kohn, Phys. Rev. 136, B 864 (1964).
[7]In the original construction of Hodges and Stott (Ref. 5), the electron density is discontinuous across atomic cell boundaries at the end of step (ii). Within the context of the energy-density functional formalism in which their theory was formulated, such a discontinuity of the electron density induces troubles, except in the simplest case of local-energy-density functional. To avoid that, we have modified step (i) in such a way as to come out with an electron density that, at the end of step (ii) is continuous across cell boundaries.
[8]C. D. Gelatt, Jr., Ph.D. thesis (Harvard Univ., Cambridge, Mass., 1974) (unpublished).
[9]L. Pauling, *The Nature of the Chemical Bond* (Cornell Univ., Ithaca, N.Y, 1960).
[10]J. A. Alonso and E. Santos, J. Phys. Chem. Solids 38, 307 (1977).
[11]J. A. Alonso and L. A. Girifalco, J. Phys. Chem. Solids 38, 869 (1977).
[12]J. A. Alonso and L. A. Girifalco, J. Phys. Chem. Solids 39, 79 (1978).
[13]R. Nieminen and C. H. Hodges, J. Phys. F 6, 573 (1976).
[14]A. R. Williams and N. D. Lang, Phys. Rev. Lett. 40, 954 (1978).
[15]D. Pettifor, J. Phys. F 7, 613 (1977).
[16]Y, Tc, and Ag are from Ref. 15. V is from D. A. Papaconstantopoulos, J. A. Anderson, and J. W. McCaffrey, Phys. Rev. B 5, 1214 (1972). Nb is from J. R. Anderson, D. A. Papaconstantopoulos, J. W. McCaffrey, and J. E. Schirber, Phys. Rev. B 7, 5115 (1973).
[17]A. R. Williams (private communication).
[18]W. Hume-Rothery, *Phase Stability in Metals and Alloys*, edited by P. S. Rudman, J. Stringer, and R. I. Jaffee (McGraw-Hill, New York, 1967).
[19]R. Boom, F. R. deBoer, and A. R. Miedema, J. Less Common Met. 45, 237 (1976).
[20]D. A. Papconstantopoulos, L. I. Boyer, B. M. Klein, A. R. Williams, V. L. Moruzzi, and J. F. Janak, Phys. Rev. B 15, 4221 (1977).
[21]R. Boom, F. R. deBoer, and A. R. Miedema, J. Less Common Met. 46, 271 (1976).
[22]H. B. Michaelson, IBM J. Res. Dev. 22, 72 (1978).
[23]P. Beck, J. Darby, and O. Arora, Trans. A. I. M. E. 206, 148 (1956); T. Philip and P. Beck, Trans. A. I. M. E. 209, 1269 (1957).
[24]J. Giner, F. Brouers, F. Gautier, and J. Van der Rest, J. Phys. F 6, 1281 (1976).
[25]J. Yamashita and S. Asano, Prog. Theor. Phys. 48, 2119 (1972).
[26]D. Papaconstantopoulos, Phys. Rev. B 11, 4801 (1975).
[27]A. R. Miedema, R. Boom, and F. R. deBoer, J. Less Common Met. 41, 283 (1975).
[28]L. Brewer, J. Nucl. Mater. 51, 2 (1974) and references therein.
[29]J. Yamashita, S. Wakoh, and S. Asano, J. Phys. Soc. Jpn. 21, 53 (1966).
[30]V. L. Moruzzi, A. R. Williams, and P. Marcus, *Charge Transfer and Electronic Structure of Alloys*, edited by L. H. Bennett and R. H. Willens (A. I. M. E., New York, 1974), p. 149.
[31]V. L. Moruzzi, A. R. Williams, and J. Janak, Phys. Rev. B 10, 4856 (1974).
[32]R. E. Watson, J. Hudis, and M. L. Perlman, Phys. Rev. B 10, 4856 (1974); T. S. Chou, M. L. Perlman, and R. E. Watson, Phys. Rev. B 14, 3284 (1976); see also, C. D. Gelatt and H. Ehrenreich, Phys. Rev. B 10, 398 (1974).